Characterization of Non-Infectious Virus-Like Particle Surrogates for Viral Clearance Applications

Sarah Johnson, Kurt A. Brorson, Douglas D. Frey, Arun K. Dhar & David A. Cetlin

Applied Biochemistry and Biotechnology
Part A: Enzyme Engineering and Biotechnology

ISSN 0273-2289

Appl Biochem Biotechnol
DOI 10.1007/s12010-017-2447-y

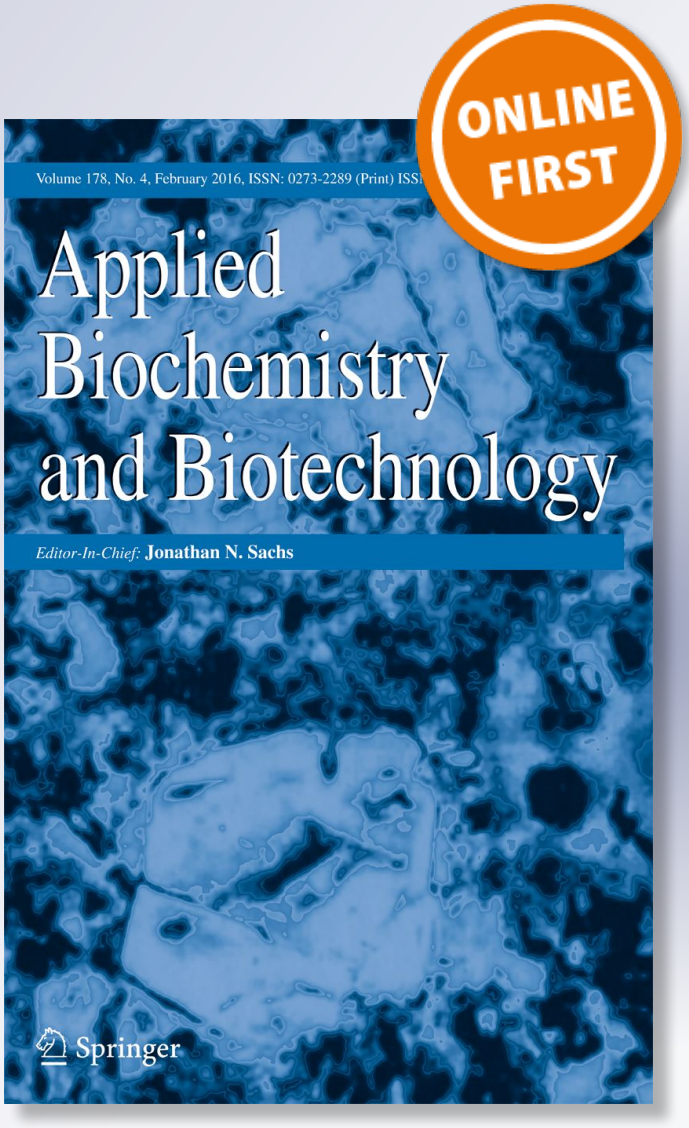

Springer

Appl Biochem Biotechnol
DOI 10.1007/s12010-017-2447-y

Characterization of Non-Infectious Virus-Like Particle Surrogates for Viral Clearance Applications

Sarah Johnson[1] · **Kurt A. Brorson**[1] · **Douglas D. Frey**[2] · **Arun K. Dhar**[3] · **David A. Cetlin**[3]

Received: 28 November 2016 / Accepted: 20 February 2017

Abstract Viral clearance is a critical aspect of biopharmaceutical manufacturing process validation. To determine the viral clearance efficacy of downstream chromatography and filtration steps, live viral "spiking" studies are conducted with model mammalian viruses such as *minute virus of mice* (MVM). However, due to biosafety considerations, spiking studies are costly and typically conducted in specialized facilities. In this work, we introduce the concept of utilizing a non-infectious MVM virus-like particle (MVM-VLP) as an economical surrogate for live MVM during process development and characterization. Through transmission electron microscopy, size exclusion chromatography with multi-angle light scattering, chromatofocusing, and a novel solute surface hydrophobicity assay, we examined and compared the size, surface charge, and hydrophobic properties of MVM and MVM-VLP. The results revealed that MVM and MVM-VLP exhibited nearly identical physicochemical properties, indicating the potential utility of MVM-VLP as an accurate and economical surrogate to live MVM during chromatography and filtration process development and characterization studies.

Keywords Viral clearance · Bioprocess development · Quality by Design · Minute virus of mice · Virus-like particle · Chromatofocusing · Chromatography · Virus filtration

*This article reflects the views of the author and should not be construed to represent FDA's views or policies.

✉ David A. Cetlin
dcetlin@mockvsolutions.com

[1] DBRRII, Office of Biotechnology Products, Office of Pharmaceutical Quality, Center for Drug Evaluation and Research, Food and Drug Administration, Silver Spring, MD 20993, USA

[2] Department of Chemical, Biochemical, and Environmental Engineering, University of Maryland Baltimore County, Baltimore, MD 21250, USA

[3] MockV Solutions, Inc., 22 Baltimore Road, Rockville, MD 20850, USA

Published online: 09 March 2017

Introduction

Viral contamination is an inherent risk to biopharmaceutical manufacturing. Sources of contamination have been traced to raw materials of animal origins or adventitious introduction during production [1]. Additionally, mammalian cells—the predominant cell type used for recombinant biopharmaceutical production—produce endogenous retroviral-like particles [1]. These risks jeopardize the safety of resulting therapeutic products such as antibodies and other therapeutic proteins. Thus, the FDA and other international regulatory agencies require viral clearance studies to validate the efficacy of downstream manufacturing processes at removing or inactivating virus prior to awarding approval for clinical or commercial use [1, 2].

Currently, viral clearance is assessed by introducing an infectious mammalian virus into a scaled-down model of a downstream manufacturing process and analyzing the ability of individual purification step at removing or inactivating the virus [3]. These live virus spiking studies are costly, require heightened safety considerations (at least biosafety level 2) with specialized personnel. They are also logistically challenging and time-consuming. As a result, downstream manufacturing processes are often developed and optimized for years with little assessment or understanding of viral clearance efficacy. This delayed approach proves risky as manufacturing processes may ultimately fail to achieve viral clearance benchmarks, potentially impacting regulatory approval for therapeutic clinical trials or commercial launch.

Cost-effective, accurate, and non-infectious viral surrogates, utilized during small-scale process development, could provide bench-top process development scientists with a unique tool to generate viral clearance data. With a quality by design approach, scientists could confidentially optimize their purification steps to remove virus and determine if process steps are effective before investing significant resources in regulatory-supporting viral clearance validation spiking studies. For over a decade, bacteriophage have been assessed as cost-effective spiking alternatives [4], but due mainly to surface physicochemical differences between them and the live mammalian virus models they seek to represent, their use has been limited mainly to size exclusion-based modes of separation (i.e., viral filtration) [5].

In this paper, we propose a new approach to viral clearance spiking studies through the novel use of virus-like particles (VLPs). VLPs are non-infectious, multi-protein structures that convey the characteristics, organization, and conformation of native infectious viruses [6], making them ideal for use as biosafety level-1 compatible spiking surrogates. Earlier studies have shown that recombinant expression of virus capsid proteins can self-assemble into VLPs that maintain the characteristics of their viral source [7]. These VLPs have been produced for potential use as vaccines [8, 9]. In this study, we generated non-infectious VLPs of *minute virus of mice* (MVM), a common parvovirus model used to demonstrate viral clearance [10], through the recombinant expression of MVM's major capsid protein, VP2 in a baculovirus/Sf9 expression system.

Viral clearance in bioprocessing operations is often accomplished through the incorporation of chromatography-based purification steps that retain viral particles while allowing the flow-through of product [11]. Retention of virus is theorized to occur through the surface interaction between particle and solid phase (chromatography resin or membrane). Data indicates that both electrostatic and hydrophobic interactions may play augmented roles in retention [12–20]. We therefore examined and compared the surface characteristics of our MVM-VLP to infectious MVM through chromatofocusing [20] and hydrophobic interaction chromatography–high-

pressure liquid chromatography (HIC-HPLC) [14] techniques. In addition, we tested and compared the surface characteristics of two bacteriophage model species, ΦX 174 and PP7.

Size-based separation techniques, such as virus filtration (i.e. nanofiltration), are also relied upon for downstream viral clearance. These removal techniques depend primarily on the physical size of molecules. We therefore examined and compared the physical characteristics of MVM-VLP to live MVM and bacteriophage through light scattering and transmission electron microscopy (TEM) techniques [21, 22]. A strong physicochemical correlation between non-infectious MVM-VLP and infectious MVM could indicate the utility of MVM-VLP and provide scientists with an accurate and practical surrogate to economically predict viral clearance during biopharmaceutical process development and optimization.

Methods

MVM-VLP Production

Non-infectious MVM-VLPs were assembled to resemble MVM. First, the MVM major capsid protein gene (VP2) was synthesized from a published MVM VP2 sequence template. Certain codons were optimized during synthesis to increase the efficiency of translation. The sequence was inserted into a cloning vector, pUC57, from which it was then subcloned into a pFastBac expression vector. This vector was then used to transform DH10Bac cells. After screening for positive clones, bacmid DNA was used to transfect Sf9 insect cells. Recombinant baculovirus carrying the MVM VP2 gene was collected from Sf9 cell culture supernatant. The original recombinant baculovirus stock was then amplified and collected 4 days post-infection. Sf9 cells were cultivated in Grace's medium supplemented with 10% FBS to a density of 5×10^5 cells/mL and then infected with amplified virus at a multiplicity of infection of 4.0. Cells were then harvested 3 days post-infection. Harvested cells were resuspended in lysis buffer (50 mM Tris-Cl, pH 7.9, 150 mM NaCl, 0.2% Triton X-100, 1 mM EDTA, and 0.5 M PMSF). This suspension was then lysed by three freeze-thaw cycles. Soluble lysate was recovered by centrifugation at 10,000*g* for 15 min in a SS34 rotor. Purification was accomplished according to the methods previously described [7]. In short, the resulting solution was first centrifuged in a 20% sucrose cushion at 35,000*g* in a Ti45 rotor/18 h/5 °C and then through a 10–40% sucrose gradient (68,000*g* in a SW41 rotor/12 h+/5 °C). Finally, fractions containing MVM-VLP (according to SDS-PAGE with Ponceau S staining and Western blot) were further separated through a CsCl gradient at the density of 1.38 g/mL (150,000*g* in SW41 rotor/48 h/10 °C). Fractions containing MVM-VLP, according to SDS-PAGE with Coomassie Blue staining, were pooled and dialyzed in a formulation buffer.

MVM Production

MVM stocks were kindly provided by Texcell North America, Inc. (Frederick, MD, USA).

Bacteriophage Production

Bacteriophages PR772, PP7, and ΦX 174 were purchased from ATCC (ATCC catalog nos. BAA-769-B1; 15,692-B4; and 13,706-B1, respectively). The corresponding host bacteria *Escherichia coli* K-12, *Pseudomonas aeruginosa*, and *E. coli* C were also purchased from

ATCC (ATCC catalog nos. BAA-769; 15,692; and 13,706 respectively). PR772 was propagated, purified, and quantified by standard plaque-forming assays as described [23]. ΦX 174 and PP7 were propagated, purified, and quantified by standard plaque-forming assays as described [24].

TEM

Negative staining TEM was utilized to quantify and measure MVM and MVM-VLP samples. Three-hundred mesh copper grids, coated with formvar and carbon, were rinsed with 0.01% bovine serum albumin, and excess solution was wicked off with filter paper. MVM- or MVM-VLP-containing samples were diluted 1:2 in PBS, and 2-μL aliquots were placed on separate grids to allow to air dry. After 10 min, residual material was wicked from grids. Samples were then fixed and stained with 20 μL of 2.0% phosphotungstic acid, which was placed onto each grid and allowed to incubate for 60 s. Excess stain was removed with filter paper. The samples were then examined using a FEI Tecnai Spirit twin transmission electron microscope, at high magnification with 80 kV. Numerous areas from each grid were examined at a minimum magnification of ×165,000 before digital images were captured.

For quantification of particles, 18 μL of MVM or MVM-VLP sample was mixed with an equal volume of latex sphere standard containing solution in microcentrifuge tubes (110-nm-diameter latex spheres, 3.0×10^{10} particles/mL). The sample/latex sphere mixture was then diluted 1:10 in ultrapure water in a separate microcentrifuge tube, vortexed, and resuspended throughout. A 2-μL aliquot of each sample/latex sphere mixture was placed on separate grids and allowed to completely air dry. Samples were then fixed, stained, and examined by TEM as described above.

Enzyme-Linked Immunosorbent Assay

An enzyme-linked immunosorbent assay (ELISA) was developed to measure the content of MVM or MVM-VLP in solution. First, samples were applied to the wells of a microwell strip (coated with guinea pig anti-MVM-VLP polyclonal antibody, MockV Solutions, Rockville, MD, USA). After incubating at 37 °C for 30 min, wells were washed with PBS + T20 three times. Then, a biotinylated version of the polyclonal capture antibody was added, and the strips were incubated and washed (as previously described). Next, horseradish peroxidase-conjugated streptavidin (Jackson ImmunoResearch Laboratories, West Grove, PA, USA) was added to the wells, and the strips were incubated and washed (as previously described). TMB substrate solution (BioFX; SurModics IVD, Eden Prairie, MN, USA) was then added to the wells, and the reaction was stopped after 3–4 min by addition of a stop solution (4% maleic acid). Optical density (OD) was then measured at 450 nm with a reference filter of 650 nm (BioTek ELx800; Winooski, VT, USA). In some cases, samples were first added into 300-kDa spin column and spun at ~5000*g* for 15 s to separate intact particles from free VP2 protein.

Buffer Preparation

Pre-made 1.0 M Tris, pH 7.5 buffer was obtained from Alfa Aesar (Ward Hill, MA, USA). Sodium chloride, sodium hydroxide, hydrochloric acid, and citric acid were obtained from Fisher Scientific (Somerset, NJ, USA). 3-(N-morpholino) propanesulfonic acid (MOPS), 3-(N-morpholino) ethanesulfonic acid (MES), glutaric acid, pyroglutamic acid, and sodium citrate

dihydrate (≥99% FG) were obtained from Sigma-Aldrich (St. Louis, MO, USA). All buffers were prepared using deionized water and were degassed by vacuum filtering using 0.22-μm polyethersulfone filter flasks (Nalgene Nunc Intl., Rochester, NY, USA). Buffers were titrated to target pH with NaOH or HCl.

Chromatofocusing

A 250 × 4-mm ProPac WCX-10 weak-base cation-exchange column was purchased from Dionex (Sunnyvale, CA, USA). Chromatofocusing experiments were performed using an Agilent 1260 HPLC equipped with a multi-array diode UV-Vis detector. An Akta in-line pH meter was connected via the Applied Biosystems Fitting Adaptor Kit (catalog no. 1–9532-00) to the UV detector via the flow cell. The Akta in-line pH probe was connected to a Jenco pH meter calibrated daily during operation. Data monitoring was performed via a virtual interface with LabView Full Development System software v2015. The chromatography systems were set up to deliver two buffers at a constant flow rate of 1.0 mL/min. The column was first equilibrated for 30–45 min with pre-saturation buffer until the pH stabilized at the buffer pH. The bacteriophage PP7 samples were passed through a 0.22-μm syringe filter before automated injection by the Agilent 1260 HPLC autosampler. For analysis, 25 μg of MVM-VLP, 1×10^9 infectious particles of MVM, or 1×10^9 PFU bacteriophage was buffer exchanged through Amicon Ultracel 30K centrifugal filters and then injected onto the column. After equilibration, the buffer was changed to 100% elution buffer while simultaneously injecting the sample onto the column. Elution buffer was allowed to flow for 10 min until elution buffer pH was obtained. Data monitoring and analysis for the Agilent HPLC were performed using the Agilent ChemStation Software version *Rev.C.01.07[27]* included with the equipment (Agilent, Santa Clara, CA, USA). The following parameters were tracked: system pressure, time, pH, UV absorbance (280 nm), conductivity, and fraction numbers. For PP7, PR772, and MVM-VLP, a UV alarm was set to collect fractions that had an absorbance ≥10 mAU. For MVM, due to low A280-nm UV signal, fractions were collected every minute. Prior to chromatofocusing of the MVM-VLPs and MVM, system qualification of the Agilent HPLC system was performed by conducting prototype runs with the PP7 and PR772 bacteriophage and comparing the results to previously published results [25].

Solute Surface Hydrophobicity Assay

A custom-designed relative hydrophobicity assay was conducted on a Tosoh TSK Phenyl 5PW column (Tosoh Biosciences, LLC) and an Agilent 1260 HPLC equipped with a multi-array diode UV-Vis detector. HPLC buffer components were purchased from Sigma-Aldrich. The Tosoh TSK Phenyl 5PW column system was run using gradients of two mobile phase buffers modified from Johnson et al. 2016 [5]. Buffer A was 0.5 M sodium citrate in 10 mM Tris, pH 8.0. Buffer B was 10 mM Tris, pH 8.0. After injection of $\geq 1 \times 10^{11}$ PFUs of bacteriophage PP7, $\geq 1 \times 10^7$ infectious MVM particles, or 25 μg of MVM-VLP, a step gradient was operated at a volumetric flow rate of 0.750 mL/min for 35 min from 100% buffer A to 100% buffer B. Note that the MVM load ($\geq 1 \times 10^7$ infectious particles) was the maximum allowable based on instrument injection volume. As a system suitability test, a series of model proteins from the GE Gel Filtration low and high molecular weight calibration kits (product codes 28–038-41, 28–038-41) were also analyzed with 250 μg injected onto the column. PP7 was also utilized as a known model virus based on data from Johnson et al. 2016.

Hydrophobicity Calculations

Relative hydrophobicity values were derived by first dividing the retention time of the solutes in the gradient by the corresponding salt concentrations. This value was then normalized to the protein standard with the lowest hydrophobicity based on this value, ribonuclease A (RNAse A). From this calculation, the solutes were ranked on a relative hydrophobicity ranking in a simple 0–1 scale, with zero being the lowest and one being the greatest hydrophobicity observed at zero salt molarity. The relative ranking of hydrophobicity for the standards was then verified with previous report [26–28].

Size Exclusion Chromatography–Multi-Angle Light Scattering

Size exclusion chromatography–multi-angle light scattering (SEC-MALS) was performed using Agilent 1200 series HPLC equipped with a TSK-GEL G3000SWXL column (7.8 × 300 mm, 5 μm; Tosoh Biosciences) and a UV detector. MALS, quasi-elastic light scattering (QELS), and refractive index (RI) measurements were achieved with a MiniDawn Treos, a Wyatt QELS, and an Optilab T-rEX, respectively (all from Wyatt Technology, Santa Barbara, CA, USA). For analysis, 25 μg of MVM-VLP, 1×10^9 infectious particles MVM, or 1×10^9 PFU of bacteriophage PP7 was buffer exchanged through Amicon Ultracel 30K centrifugal filters and then injected onto the column and analyzed at a flow rate of 0.4 mL/min. Signals were processed using ASTRA software package (version 6.1) (Wyatt Technology) to calculate the hydrodynamic radius using a refractive index increment (dn/dc) value of 0.185 mg/g.

Results

Physical Characterization

TEM and SEC-MALS

The efficacy of nanofiltration-based virus removal relies predominantly on the physical separation of viral particles from protein of interest. The major contributing factor to efficient removal by filtration is viral particle diameter. TEM imaging after negative staining is a technique used to quantitatively measure viral particle diameter and qualitatively analyze their morphology, although staining procedures can shrink or swell viral particle size [23]. Through this technique, both infectious MVM and MVM-VLP were shown to be fully formed spherical particles (Fig. 1), containing radii of 12.3 ± 1.8 and 12.8 ± 1.5 nm, respectively (Table 1). The radius of MVM reported here is near the range of previously reported results [16, 29]. Reference values for bacteriophage PP7 and ΦX174 were also included in Table 1.

SEC-MALS, a technique that has been used in determining the hydrodynamic radius of viral particles, was also performed. While the hydrodynamic radius of a virus or VLP measured by SEC-MALS may be a higher estimate from the diameter/radius measured by TEM, it is highly reflective of the actual particle translational behavior in the fluid. Through this technique, native MVM and MVM-VLP were determined to have hydrodynamic radii of 17.7 ± 0.2 and 17.2 ± 0.0 nm, respectively

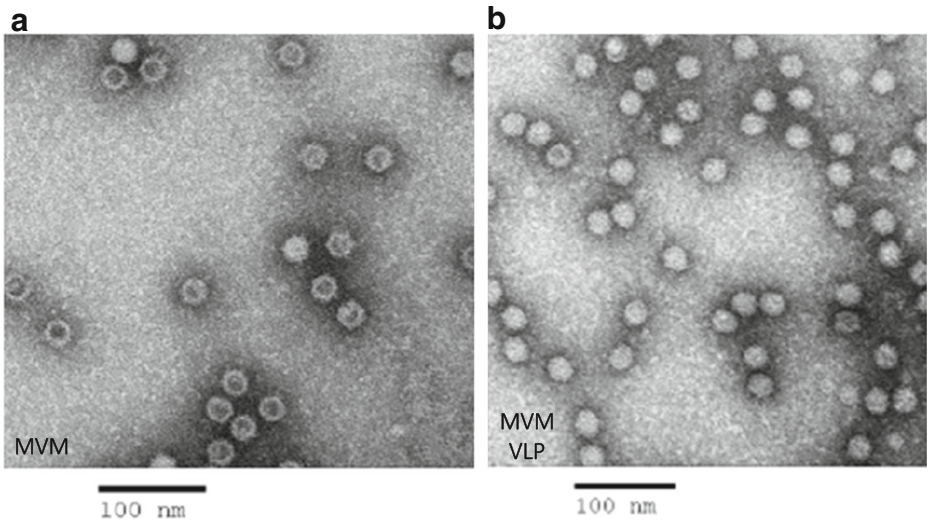

Fig. 1 Transmission electron microscopy (TEM) images of viral particles at ×110,000 magnification after negative staining. **a** Infectious MVM. **b** MVM-VLP. Particles of each species were found to be overall intact and evenly distributed. The *darker area* within some infectious MVM and MVM-VLP particles is thought to be caused by dye penetrating into the structure

(Table 1), while bacteriophage PP7 was determined to have a hydrodynamic radius of 16.9 ± 0.1.

Surface Characterization

Surface Charge

The isoelectric point (pI) of a virus particle can impact its partitioning on ion exchange chromatography unit operations [20, 30]. The true isoelectric point (pI_{actual}) of MVM has previously been estimated by chromatofocusing techniques to be 6.2 ± 0.5 pH units [20]. We performed a similar series of chromatofocusing experiments using a weak cation exchanger to confirm this value and to determine the pI_{actual} of MVM-VLP. Because mammalian virus preparations have titer concentrations which are generally insufficient to generate strong A_{280} traces [20], we tracked MVM elution by collecting fractions throughout each run and analyzed their content via ELISA. In contrast, the highly purified MVM-VLP preparation generated a

Table 1 Size-based comparison of particles from multiple methods

Particle species	TEM radii (nm)	SEC-MALS hydrodynamic radii (nm)
Infectious MVM	12.3 ± 1.8	17.7 ± 0.2
MVM-VLP	12.8 ± 1.5	17.2 ± 0.0
PP7	13[a]	16.9 ± 0.1
ΦX174	14.5 ± 1.5[a]	ND

[a] Value was derived from reported electron microscopy diameters [22]. For SEC-MALS, ± indicates the statistical consistency of the hydrodynamic radius calculation from mathematical models within the Astra software (not absolute error)

ND no data available

strong, monolithic A_{280} peak during the linear portion of the pH gradient and a minor peak during the void volume. We collected this strong main peak and the minor peak void volume samples and confirmed the presence of the MVM-VLP via ELISA.

The pH at which intact infectious MVM or MVM-VLP eluted from the column (pI_{app}) was determined (Table 2) and used to calculate pI_{actual} through a previously established model based on a multiple-charge state (MCS) representation [20, 25]. In general, the mathematical model developed by Shen and Frey in 2004 [31] utilizes the elution pH and retention time of a solute from several chromatographic runs with different mobile phase salt concentrations to estimate the true isoelectric point of the solute (Fig. 2a–d). With the exception of the 100 mM NaCl condition for MVM, pI_{app} values for both MVM and the MVM-VLP decreased with increasing salt concentrations, a phenomenon previously shown to occur for MVM [20]. According to the MCS model previously described by Brorson et al., this behavior indicates that these particles exhibit a low dependence of net charge on pH (i.e., a low value for dz/dpH) at their true isoelectric points. In this case, the calculation of pI_{actual} from the MCS model is expected to be reasonably accurate. Using this model, the pI_{actual} values of MVM and MVM-VLP were calculated to be 5.99 and 5.81, respectively, confirming the slightly acidic pI_{actual} of MVM previously reported and demonstrating close comparability for this important attribute between MVM and the MVM-VLP. As a benchmark for the method, the bacteriophage PP7 was also tested at varying salt concentrations (Table 2) and found to be more acidic than MVM, confirming results previously reported [25]. Another observation consistent with previous reporting [25] was that the dz/dpH value exhibited by PP7 indicates that the MCS model does not fit. For PP7, pI_{actual} can be estimated to be within the range of measured pI_{app} values, i.e., 4.84–4.98.

Surface Hydrophobicity

The hydrophobicity of a virus has been shown to impact purification in hydrophobic interaction [32, 33] or multi-modal chromatography unit operations [34]. We utilized a novel hydrophobicity assay adapted for phage and viruses [14, 34] to determine and compare the relative surface hydrophobicity of infectious MVM and MVM-VLP. This assay is a modification from a hydrophobic interaction chromatography-based technique typically used for proteins, which has recently demonstrated utility in resolving several bacteriophage particles as well as model therapeutic antibodies in comparison to known protein standards [14, 34]. In general, the higher the hydrophobicity of the solute is, the higher the required

Table 2 Chromatofocusing data of infectious MVM, MVM-VLP, and the bacteriophage PP7 at various salt concentrations

Particle species	Salt concentration (mM NaCl)	pI_{app}	pI_{actual}
Infectious MVM	0	6.33	5.99
	10	6.18	
	50	5.47	
	100	5.79	
MVM-VLP	0	6.13	5.81
	10	5.85	
	50	5.51	
	100	5.13	
PP7	0	4.98	4.74
	50	4.87	
	100	4.84	

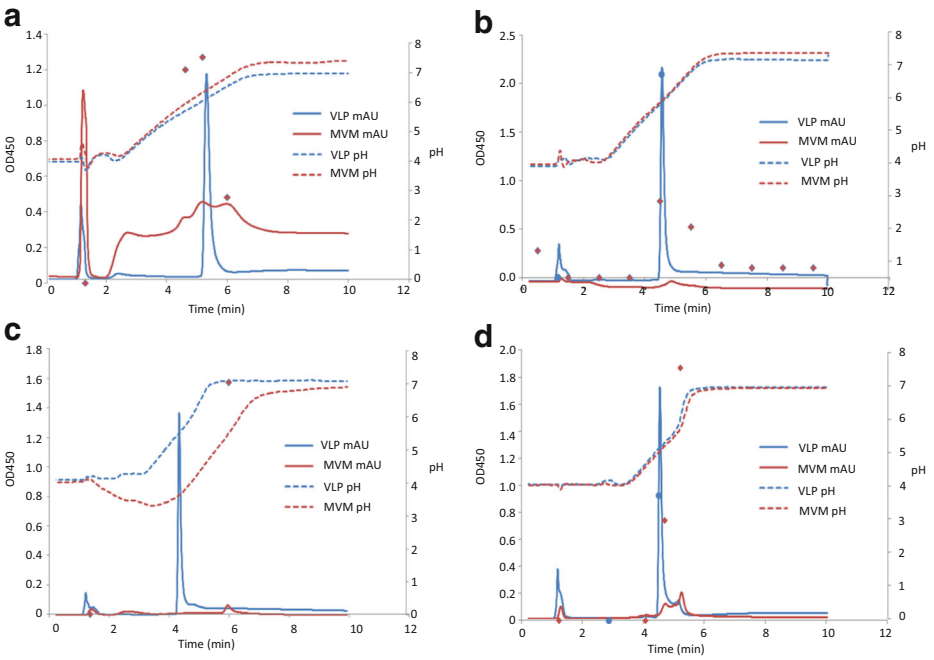

Fig. 2 Chromatogram and ELISA OD_{450} result overlays of MVM and MVM-VLP experiments at various NaCl concentrations. **a** 0 mM NaCl. **b** 10 mM NaCl. **c** 50 mM NaCl. **d** 100 mM NaCl. Absorbance at 280 nM (mAu) data captured during each MVM (*red solid line*) and MVM-VLP (*blue solid line*) is plotted (no *y* axis) along with respective pH gradients (*red dotted line* for MVM, *blue dotted line* for MVM-VLP) (*right y* axis). Overlaying each chromatogram is ELISA OD_{450} data (*left y* axis) for MVM (*red diamond*) and MVM-VLP (*blue circle*). Note that MVM-VLP ELISA data was not obtained for 0- and 50-mM runs

concentration of salt for elution off the column is. Each solute was given a "relative hydrophobicity" value based on its eluting salt concentration normalized to the salt concentrations of protein standards eluting within the same operating system (see "Methods" section for details). After MVM or MVM-VLP-containing preparations were applied to a Tosoh TSK Phenyl 5PW column, a mobile phase gradient of high salt (0.5 M citrate) to no salt (0.0 M citrate) was applied. Particles eluted from the column according to their hydrophobicity (less hydrophobic particles eluting early and more hydrophobic particles eluting later). Although the MVM-VLP preparation produced traceable A_{280} signal on the Agilent 1260 HPLC, the MVM preparation did not. This is a consistent phenomenon seen previously with MVM [20]. Nevertheless, fractions of each species were collected throughout the gradient and analyzed via ELISA. These results verified that MVM-VLP elution corresponded with the visible UV peak (around 11.3 min into the gradient). The citrate concentration at this point was 144 mM. The ELISA results also determined that peak MVM elution occurred around 10.5 min, corresponding with a very similar citrate concentration of 158 mM (Fig. 3a). Comparing these values to several model protein standards (Fig. 3b), MVM and MVM-VLP score relative hydrophobicity values of 0.28 and 0.35, respectively, indicating that MVM is modestly hydrophobic and slightly less so than the corresponding MVM-VLP. In comparison, PP7 and ΦX174 bacteriophages, commonly used as a surrogate for MVM in size-based applications, were previously analyzed and determined to have relative hydrophobicity values of 0.61 and 0.18, respectively (Fig. 3b), indicating that their surfaces differ in hydrophobicity to MVM, ΦX174 being less hydrophobic and PP7 being more hydrophobic.

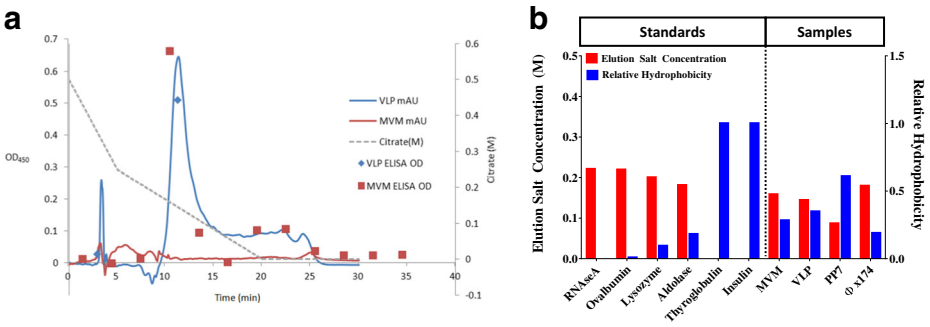

Fig. 3 HIC chromatogram overlay with ELISA OD_{450} results. **a** Citrate concentration (represented by the *dotted line*) decreased stepwise throughout infectious MVM and MVM-VLP experiments (*right y* axis). As citrate decreased from the column, eluting particles generated a visible UV signal for infectious MVM (*red trace*) and MVM-VLP (*blue trace*) (*y* axis not shown). Fractions collected during the experiments were analyzed via ELISA. ELISA OD_{450} data for MVM (*red square*) and MVM-VLP (*blue diamond*) are shown overlaying the chromatogram (*left y* axis). **b** Relative hydrophobicity values. Protein standards and test article samples (infectious MVM, MVM-VLP ("VLP"), PP7, ΦX174) are plotted according to the salt concentration at which they were determined to elute from the HIC column (*red*). Samples are also plotted according to their relative hydrophobicities (*blue*) as determined through comparison to the protein standards

Discussion

The logistics and high costs of evaluating viral clearance are major limitations during downstream biopharmaceutical process development and characterization. Recognizing the high costs incurred during viral clearance validation, efforts have been made to incorporate viral clearance into process design at earlier developmental stages through the utilization of lower-cost viral surrogates. Early studies involving the use of bacteriophage as spiking agents proved useful when evaluating nanofiltration process steps and led to the standardization of nomenclature used for virus-retentive filters [21, 22]. Although physical comparisons between certain bacteriophage and model mammalian viruses such as MVM justify their use for size-based nanofiltration applications, uncertainties surrounding surface properties have given scientists pause concerning their use in evaluating chromatographic modes of separation [5, 35]. Recent work shows that the surface characteristics of virus particles are important considerations when designing process parameters for biopharmaceutical products that rely on electrostatic [20, 30], hydrophobic interaction [22, 23], or multi-modal mechanisms [20] of separation.

We have chosen to explore another class of surrogates, VLPs, which may provide an economical and accurate method for predicting viral clearance through any mode of separation. VLPs are assembled from the capsid and/or envelop proteins of the live viruses and have been shown, through their use as vaccines, to maintain the key surface attributes of their source virus. It is this ability to mimic the physicochemical properties of live viruses which make VLPs promising spiking surrogates for viral clearance studies. We examined and compared the size, surface charge, and surface hydrophobicity characteristics of MVM-VLP to live MVM. In addition, we examined and compared two bacteriophage species, ΦX-174 and PP7, typically used as size-based surrogates for MVM.

The diameter of live MVM has been reported throughout the decades of its study and, depending on analytical technique and preparation, is accepted to comprise a diameter of 20–26 nm [29]. The first reported measurements utilized TEM; however, since then, light-

scattering techniques (e.g., DLS, MALS) have become important tools for determining the sizes and distributions of viruses and VLPs. These techniques offer the ability to study virus particles in a more native state than TEM. Through SEC-MALS, we measured the hydrodynamic radius of MVM to be in the range of 17.7 ± 0.2 nm, implying a viral diameter of ~36 nm. In comparison, MVM-VLP was measured to possess a hydrodynamic radius of 17.2 ± 0.0 nm, implying a viral diameter of ~34 nm. Some imprecision in analysis may be due to the particles residing in or below the lower limit of the analytical technique's accuracy range, but it is known that light-scattering measurements typically provide high-end estimates for particle size as the native particles analyzed remain in a fluid state [36]. In contrast, TEM is known to be a low-end estimate due to particle shrinkage during sample preparation [23]. As such, data presented here is most useful for comparative purposes than as a benchmark value for absolute size. Traditional TEM-based results placed MVM's diameter between 21.0 and 28.2 nm, comparable to established ranges [29]. MVM-VLP diameter was found to be in the range of 22.6–28.6 nm. It is clear to see through both types of physical analysis that the dimensions of live MVM and MVM-VLP are very similar. Historical TEM measurements show bacteriophage ΦX-174 to possess a diameter ranges of 26.0–32.0 nm [22], slightly larger than either MVM or MVM-VLP. This data may suggest that for physical modes of separation, MVM-VLP could be a more precise, size-based MVM surrogate than ΦX-174.

Recent advances in the technique of chromatofocusing and in the development of mechanistic models for predicting isoelectric points from chromatographic retention times have made possible the measurement of inherent virus particle surface charge, a property which governs a particle's dynamic interaction with solid phase-charged groups as it transverses a chromatography column or membrane during separation. Previously, Strauss and collaborators [20] determined infectious MVM to have a true pI (pI_{actual}) of 6.2 while utilizing a chromatofocusing technique with a fast protein liquid chromatography (FPLC) system and a sophisticated model based on representing the virus as a multiple set of charge states, which distribute between phases in equilibrium. Our results (pI_{actual} = 5.99), generated on a HPLC system, were very similar and not only confirmed the slightly acidic nature of native MVM but may represent a more refined value due to the higher resolution potential of HPLC over FPLC. MVM-VLP chromatofocusing at various salt concentrations revealed a pI_{actual} value of 5.81, slightly more acidic but very similar to live MVM. In contrast, the benchmark bacteriophage MVM surrogate, PP7, exhibited consistently lower pI_{app} values at various salt conditions, which did not allow for calculation of a precise pI_{actual} through the MCS model. A similar phenomenon for PP7 was seen previously by Brorson and collaborators [25] when utilizing the chromatofocusing technique on an FPLC. Based on these results, it would seem that for charge-based separation applications, the MVM-VLP could serve as a more accurate marker for MVM prediction than the acidic PP7 bacteriophage.

Depending on the mode of separation, hydrophobic interactions often play a leading or supporting role during the purification of a therapeutic protein from impurities or contaminants such as virus particles. One relatively newer mode of separation in which hydrophobic interactions play a role in resolution is mixed-mode chromatography. Mixed-mode chromatography resins are quickly gaining prominence in biomanufacturing processes due to their salt tolerance and the potential of cost savings incurred from column step reduction [37–39]. Preliminary work with mixed-mode chromatography indicates that particle hydrophobicity is now an important consideration for viral clearance when designing chromatography unit operations [34]. Additionally, hydrophobic interactions may play minor, unintentional roles during ion exchange, affinity, or even sized-based separations as interactions with base

matrices or other molecules present in solution are possible. For these reasons, a fundamental understanding of the hydrophobic properties of virus particles is an important step toward methodically optimizing conditions for their removal.

Through the advent of an analytical hydrophobicity assay, we have determined the point at which native MVM particles elute from a hydrophobic surface (~160 mM citrate) and have compared this point to a panel of standard proteins to determine MVM's relative hydrophobicity. The results indicate that native MVM is mildly hydrophobic and could be resolved from other molecules present in solution depending on their own relative hydrophobicity. Preliminary work utilizing a similar assay has determined that monoclonal antibodies exhibit a range of hydrophobicity from mild hydrophobicity to high hydrophobicity [14]. More research in this area could help optimize operating conditions for viral clearance among chromatographic modes of separation that utilize hydrophobic properties.

Hydrophobicity analysis for MVM-VLP revealed a slightly lower elution citrate concentration to live MVM, indicating that the MVM-VLP exhibited a similar but slightly higher dynamic surface hydrophobicity to live MVM. In contrast, the bacteriophage PP7 was determined to exhibit a significantly lower elution citrate concentration to either MVM or MVM-VLP, which designates a higher hydrophobic surface. This finding suggests that PP7's behavior in chromatography-based applications could be governed more by hydrophobic interactions than either live MVM or MVM-VLP. Conversely, bacteriophage ΦX-174 was determined to elute at a higher citrate concentration to either MVM or MVM-VLP and, therefore, possesses a lower hydrophobic surface.

Overall, the physicochemical data gathered throughout this study indicates the potential to utilize MVM-VLP as an accurate spiking surrogate during chromatographic or filtration-based MVM clearance studies. The potential value for an accurate, non-infectious, and economical MVM surrogate could be substantial. Quality by design and design of experiment principles, applied during process development and characterization, could be extended to optimize MVM clearance operating space in much the same way that host cell protein or DNA operating spaces are defined today. Furthermore, MVM-VLP spiking experiments could be used to predict viral clearance failures earlier in development.

Acknowledgements This project was supported in part by an appointment to the Research Participation Program at FDA/CDER/OBP administered by the Oak Ridge Institute for Science and Education through an interagency agreement between the DOE and FDA. Funding was also provided by the Regulatory Science and Review Enhancement Program (RSR) 15-14 and the Research Review Coordinating Committee (RRCC).

References

1. The International Council for Harmonisation of Technical Requirements for Pharmaceuticals for Human Use: ICH Harmonised Tripartite Guideline Q5A(R1) (1999). Viral Safety Evaluation of Biotechnology Products Derived from Cell Lines of Human or Animal Origin.
2. Volkov, G. L., Havryliuk, S. P., Krasnobryzha, I. M., & Havryliuk, O. S. (2016). The protein/peptide direct virus inactivation during chromatographic process: developing approaches. *Applied Biochemistry and Biotechnology*, 1–17.
3. Darling, A. (2002). Validation of biopharmaceutical purification processes for virus clearance evaluation. *Molecular Biotechnology, 21*(1), 57–83.
4. Aranha-Creado, H., & Brandwein, H. (1999). Application of bacteriophages as surrogates for mammalian viruses: a case for use in filter validation based on precedents and current practices in medical and environmental virology. *PDA Journal of Pharmaceutical Science and Technology, 53*(2), 75–82.

5. Aranha, H., & Forbes, S. (2001). Viral clearance strategies for biopharmaceutical safety. *Pharmaceutical technology*.
6. Roldão, A., Mellado, M. C., Castilho, L. R., Carrondo, M. J., & Alves, P. M. (2010). Virus-like particles in vaccine development. *Expert Review of Vaccines, 9*(10), 1149–1176.
7. Hernando, E., Llamas-Saiz, A. L., Foces-Foces, C., McKenna, R., Portman, I., Agbandje-McKenna, M., & Almendral, J. M. (2000). Biochemical and physical characterization of parvovirus minute virus of mice virus-like particles. *Virology, 267*(2), 299–309.
8. Lin, Q., Yang, K., He, F., Jiang, J., Li, T., Chen, Z., ... & Xia, N. (2016). Production of influenza virus HA1 harboring native-like epitopes by *Pichia pastoris*. *Applied biochemistry and biotechnology*, *179*(7), 1275–1289.
9. Buonaguro, F. M., & Buonaguro, L. (2014). Virus-like particles in vaccine development. *Virus*, 2–4.
10. Gefroh, E., Dehghani, H., McClure, M., Connell-Crowley, L., & Vedantham, G. (2014). Use of MMV as a single worst-case model virus in viral filter validation studies. *PDA Journal of Pharmaceutical Science and Technology, 68*(3), 297–311.
11. Liu, H. F., Ma, J., Winter, C., & Bayer, R. (2010). Recovery and purification process development for monoclonal antibody production. *MAbs, 2*(5), 480–499.
12. Farrah, S. R., Shah, D. O., & Ingram, L. O. (1981). Effects of chaotropic and antichaotropic agents on elution of poliovirus adsorbed on membrane filters. *Proceedings of the National Academy of Sciences, 78*, 1229–1232.
13. Gerba, C. P. (1984). Applied and theoretical aspects of virus adsorption to surfaces. *Advances in Applied Microbiology, 30*, 133–168.
14. Johnson, S., Brown, M. Brorson, K and Lute, S. (2016). Developing a high-salt HIC HPLC assay to define relative hydrophobicity of viral particles, *2016 American Chemical Society BIOT Meeting*, San Diego, CA.
15. Miesegaes, G., Bailey, M., Willkommen, H., Chen, Q., Roush, D., Blumel, J., & Brorson, K. (2010). Proceedings of the 2009 viral clearance symposium. *Developmental Biology (Basel), 133*, 3–101.
16. Miesegaes, G., Lute, S., & Brorson, K. (2010). Analysis of viral clearance unit operations for monoclonal antibodies. *Biotechnology and Bioengineering, 106*, 238–246.
17. Miesegaes, G. R., Lute, S., Strauss, D. M., Read, E. K., Venkiteshwaran, A., Kreuzman, A., Shah, R., Shamlou, P., Chen, D., & Brorson, K. (2012). Monoclonal antibody capture and viral clearance by cation exchange chromatography. *Biotechnology and Bioengineering, 109*, 2048–2058.
18. Miesegaes, G. R., Lute, S. C., Read, E. K., & Brorson, K. A. (2014). Viral clearance by flow-through mode ion exchange columns and membrane adsorbers. *Biotechnology Progress, 30*, 124–131.
19. Shields, P. A., & Farrah, S. R. (1983). Influence of salts on electrostatic interactions between poliovirus and membrane filters. *Applied and Environmental Microbiology, 45*, 526–531.
20. Strauss, D. M., Lute, S., Tebaykina, Z., Frey, D. D., Ho, C., Blank, G. S., Brorson, K., Chen, Q., & Yang, B. (2009). Understanding the mechanism of virus removal by *Q* sepharose fast flow chromatography during the purification of CHO-cell derived biotherapeutics. *Biotechnology and Bioengineering, 104*, 371–380.
21. Brorson, K., Lute, S., Haque, M., Martin, J., Sato, T., Moroe, I., Morgan, M., Krishnan, M., Campbell, J., Genest, P., & Parrella, J. (2008). A consensus rating method for small virus-retentive filters. II. Method evaluation. *PDA Journal of Pharmaceutical Science and Technology, 62*, 334–343.
22. Lute, S., Riordan, W., Pease, L. F., Tsai, D. H., Levy, R., Haque, M., Martin, J., Moroe, I., Sato, T., Morgan, M., & Krishnan, M. (2008). A consensus rating method for small virus-retentive filters. I. Method development. *PDA Journal of Pharmaceutical Science and Technology, 62*, 318–333.
23. Lute, S., Aranha, H., Tremblay, D., Liang, D., Ackermann, H. W., Chu, B., Moineau, S., & Brorson, K. (2004). Characterization of coliphage PR772 and evaluation of its use for virus filter performance testing. *Applied and Environmental Microbiology, 70*, 4864–4871.
24. Lute, S., Bailey, M., Combs, J., Sukumar, M., & Brorson, K. (2007). Phage passage after extended processing in small-virus-retentive filters. *Biotechnology and Applied Biochemistry, 47*, 141–151.
25. Brorson, K., Shen, H., Lute, S., Perez, J. S., & Frey, D. D. (2008). Characterization and purification of bacteriophages using chromatofocusing. *Journal of Chromatography. A, 1207*, 110–121.
26. Kramarczyk, J. F., Kelley, B. D., & Coffman, J. L. (2008). High-throughput screening of chromatographic separations: II. Hydrophobic interaction. *Biotechnology and Bioengineering, 100*(4), 707–720.
27. Queiroz, J. A., Tomaz, C. T., & Cabral, J. M. S. (2001). Hydrophobic interaction chromatography of proteins. *Journal of Biotechnology, 87*(2), 143–159.
28. Szepesy, L., & Rippel, G. (1992). Comparison and evaluation of HIC columns of different hydrophobicity. *Chromatographia, 34*(5–8), 391–397.
29. Van Regenmortel, M., Fauquet, C., Bishop, D., Carstens, E., Estes, M., & Lemon, S. (2000). *Virus taxonomy: seventh report of the international committee on taxonomy of viruses*. San Diego: Academic Press.
30. Curtis, S., Lee, K., Blank, G. S., Brorson, K., & Xu, Y. (2003). Generic/matrix evaluation of SV40 clearance by anion exchange chromatography in flow-through mode. *Biotechnology and Bioengineering, 84*, 179–186.

31. Shen, H., & Frey, D. D. (2004). Charge regulation in protein ion-exchange chromatography: development and experimental evaluation of a theory based on hydrogen ion Donnan equilibrium. *Journal of Chromatography. A, 1034*(1–2), 55–68.
32. Steppert, P., Burgstaller, D., Klausberger, M., Kramberger, P., Tover, A., Berger, E., Nöbauer, K., Razzazi-Fazeli, E., & Jungbauer, A. (2017). Separation of HIV-1 gag virus-like particles from vesicular particles impurities by hydroxyl-functionalized monoliths. *Journal of Separation Science*. doi:10.1002/jssc.201600765.
33. Segura, M., Puig, M., Monfar, M., & Chillón, M. (2012). Chromatography purification of canine adenovirual vectors. *Human Gene Therapy Methods, 23*, 182–197.
34. Brown, M., Johnson, S., Brorson, K., Lute, S., & Roush, D. (2017). A step-wise approach to define binding mechanisms of surrogate viral particles to multi-modal anion exchange resin in a single solute system. *Biotechnology and Bioengineering*. doi:10.1002/bit.26251.
35. Miesegaes, G. R., Lute, S., Strauss, D. M., Read, E. K., Venkiteshwaran, A., Kreuzman, A., ... & Brorson, K. (2012). Monoclonal antibody capture and viral clearance by cation exchange chromatography. *Biotechnology and bioengineering*, *109*(8), 2048–2058.
36. Domingos, R. F., Baalousha, M. A., Ju-Nam, Y., Reid, M. M., Tufenkji, N., Lead, J. R., ... & Wilkinson, K. J. (2009). Characterizing manufactured nanoparticles in the environment: multimethod determination of particle sizes. *Environmental Science & Technology*, *43*(19), 7277–7284.
37. Bolton, G., & Blümel, J. (2016). Proceedings of the 2015 viral clearance symposium. Session 5: conference summary: key discussion and outcomes, pending questions, and proposed experiments. *PDA Journal of Pharmaceutical Science and Technology, 70*, 477–481.
38. Bolton, G., & Blümel, J. (2016). Session 5: conference summary: key discussion and outcomes, pending questions, and proposed experiments. *PDA Journal of Pharmaceutical Science and Technology, 70*, 477–481.
39. Brorson, K. (2016). PDA/FDA virus & TSE safety conference. *PDA Journal of Pharmaceutical Science and Technology, 70*, 93.